

Kinetic and thermodynamic analysis of proteinlike heteropolymers: Monte Carlo histogram technique

NICHOLAS D. SOCCI AND JOSÉ NELSON ONUCHIC

Department of Physics, University of California at San Diego, La Jolla, California 92093-0319

(In press *J. Chem. Phys.*)

Abstract

Using Monte Carlo dynamics and the Monte Carlo Histogram Method, the simple three-dimensional 27 monomer lattice copolymer is examined in depth. The thermodynamic properties of various sequences are examined contrasting the behavior of good and poor folding sequences. The good (fast folding) sequences have sharp well-defined thermodynamic transitions while the slow folding sequences have broad ones. We find two independent transitions: a collapse transition to compact states and a folding transition from compact states to the native state. The collapse transition is second order-like, while folding is first order. The system is also studied as a function of the energy parameters. In particular, as the average energetic drive toward compactness is reduced, the two transitions approach each other. At zero average drive, collapse and folding occur almost simultaneously; i.e., the chain collapses directly into the native state. At a specific value of this energy drive the folding temperature falls below the glass point, indicating that the chain is now trapped in local minimum. By varying one parameter in this simple model, we obtain a diverse array of behaviors which may be useful in understanding the different folding properties of various proteins.

I INTRODUCTION

Simple models are one powerful theoretical tool for the study of complex systems. The idea is to remove all but the essentials from the original system which will ideally allow for a more complete analysis. There is often a trade-off between the complexity of the model (or how faithfully it represents the system of interest) and the thoroughness of the analysis. In the case of protein folding, research has spanned the entire spectrum from all-atom molecular dynamics

with solvent^{1,2,3,4} to complete enumeration of simple lattice polymer systems,^{5,6} with many works in between these two extremes. Naturally the more realistic simulations do not yield results as thorough as the simpler ones. In the all-atoms simulations a large amount of supercomputer time is required for runs of hundreds of picoseconds of a single protein molecule (plus solvent). In contrast, high-end workstations can be used to simulate lattice polymers. Many different sequences can be simulated over a range of temperatures for time scales comparable to the folding time. We do not want to imply that one set of techniques is superior than the other, but rather in studying a system as complex as proteins many different approaches are necessary. In fact the two limits complement each other. Simple systems permit detailed analysis while the more complex systems allow for contact with real proteins. Connecting these two limits would allow for a more thorough analysis of real protein systems. Such an analysis has been recently carried out.^{7,8}

In a previous work⁹ we examined the kinetics of a simple three-dimensional lattice polymer system. This system is too large for exact enumeration studies but is still small enough for detailed analysis. Many studies of lattices models seem to focus either on thermodynamics or on kinetics, considering each in isolation. However, as previously shown⁹ and shown here, a combined approach that considers both the kinetics and thermodynamics of the same system is important in understanding the model in detail. We have determined that there is an important relation between kinetics (the “glass transition”) and thermodynamics (the folding temperature) in determining whether a sequence will fold or not, an idea that was advanced by Bryngelson and Wolynes,^{10,11} and later explored by Leopold and Onuchic.¹² In this work we continue the study of this system, examining both thermodynamics and kinetics in greater detail.

Some of the earliest work on the thermodynamics of protein-like lattice polymers has been performed by Chan, Lau and Dill.^{13,14} They examined short chains in two dimensions for which it is possible to enumerate all conformations. This allowed them to calculate any thermodynamic quantity by simply summing over states. By measuring a variety of parameters, such as the average compactness, number of contacts and hydrophobic core, they found a distinct difference between folding and non-folding sequences. Although exact enumeration studies are extremely powerful, they are limited to small chains, usually in two dimensions. In three dimensions many have studied the 27 monomer system on a simple cubic lattice which has a maximally compact shape of a $3 \times 3 \times 3$ cube. It is not possible to enumerate all conformations, but it is still possible to enumerate all *compact* conformations (what is often referred to as the *cube spectrum*) and then calculate approximate thermodynamics using just the cube states.^{15,16} However, as we show in this work, care must be taken in using this technique since the cube states are not an accurate approximation to the full density of states; in particular there are many low energy (i.e., thermodynamically relevant) states that are not cubes.

For longer chains, one can use the standard Monte Carlo technique¹⁷ for calculating thermodynamic properties. Skolnick, Sikorski and Kolinski^{18,19,20} use a dynamic Monte Carlo method to study folding of realistic protein-like structures on a diamond lattice. The word dynamic here is used to indicated that the move set has been selected in such a way that the actual time course of folding is as realistic as possible. Note that this is not necessary for calculating thermodynamic quantities, since it is only necessary that the moves satisfy detailed balance. In fact, O'Toole and Panagiotopoulos²¹ found that using the dynamic moves for the 3D cubic lattice system led to sampling problems. At low temperature they observed a hysteresis for the average energy. This is probably caused by trying to sample below the glass transition. This transition was predicted¹⁰ and explicitly shown⁹ to exist in these simple lattice systems. O'Toole and Panagiotopoulos were able to circumvent this problem by using a more sophisticated sampling procedure based on the Rosenbluth and Rosenbluth chain growth algorithm.²² They studied chains as long as 48 monomers and have used this technique to study thermodynamically significant low energy conformations.²³ Others have used Monte Carlo techniques to examine the effects of various potential functions on the kinetics and thermodynamics of two-dimensional lattice polymer systems.²⁴

These previous studies used the standard Monte Carlo technique. The simulation is run at a given temperature and various averages are computed. To obtain thermodynamic quantities for a different temperature, another simulation (at the new temperature) is performed. However, it is possible to extract information about temperatures other than the simulation temperature using a technique often called the *Monte Carlo Histogram Method*.^{25,26} Using this technique one can calculate an approximate density of states for the system, which can be used to calculate any thermodynamic quantity of interest over a range of temperatures. Because of the small system sizes used, we can obtain accurate results over a broad range of temperatures. In particular, we can extrapolate into the glass region where running normal simulations becomes extremely difficult and time consuming. The technique also facilitates the finding of peaks or zeros of various thermodynamic functions. It can be used to calculate extensive quantities like the free energy or entropy of the system, which are difficult to extract by the standard Monte Carlo procedure. One can not only vary the temperature, but also the various parameters in the potential. One can examine how the system behaves thermodynamically at a range of parameter values without the need to run new simulations. This in-depth analysis of the thermodynamics has enabled us, along with several others, to begin to connect the behavior and properties of these simple model systems with those of real proteins.^{7,8}

II MODEL AND METHODS

A Definition of model and dynamics

The model studied was a simple three-dimensional cubic lattice polymer. All chains were 27 monomers long with two different monomer types. The potential was a contact interaction between monomers that are nearest neighbors on the lattice (but that are not linked covalently). The energy of a contact was E_l for a pair of the same monomer type and E_u for a pair of different monomers. This model was the same one used in our previous study⁹ (which can be consulted for a more detailed explanation of the model). The energy function is:

$$E = N_l E_l + N_u E_u, \quad (1)$$

where N_l is the number of contacts between monomers of the same type (like contacts) and N_u the number of contacts between monomers of different types.

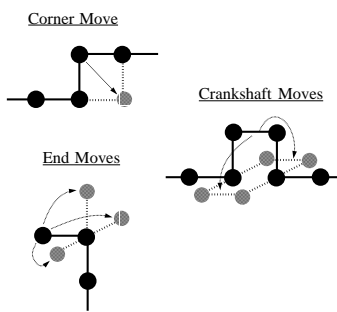


Figure 1: The three types of moves used in the simulations. The light circles represent the possible lattice points to which a given monomer can move, provided that that point is not occupied. In the case of the end and crankshaft moves, one of the possible moves is picked at random. Note that the corner and crankshaft moves are exclusive: A non-end monomer can only make one or the other depending on the position of its neighbors along the chain.

Although it is easiest to express the energy function in terms of the E_l and E_u variables, some properties of the model are more clearly understood by considering an equivalent set of parameters, E_{avg} and Δ , defined as follows:

$$\begin{aligned} E_{\text{avg}} &= \frac{1}{2} (E_l + E_u) \\ \Delta &= (E_u - E_l). \end{aligned} \quad (2)$$

E_{avg} represents the overall drive toward forming contacts or compacting the chain. If it is less than zero, contact formation will be favored. Δ determines the heterogeneity of the heteropolymer. In the limit that $\Delta = 0$ the model becomes a homopolymer. In our previous work,⁹ $E_{\text{avg}} = -2$ and $\Delta = 2$, giving values -3 and -1 for E_l and E_u respectively.²⁷ This insures that the chain collapses rapidly, compared to folding, and that the minimum energy state is a maximally compact cube for the sequences considered here. When we say the chain has folded we mean it is in the native state. This is distinguished from collapse, which refers to chains that can be in any compact conformation. The same parameters were used for part of the results presented here. In addition we show how the model behaves as these parameters are varied.

The move set is shown in figure 1 and consists of local one- or two-monomer moves. These moves are the standard set used in lattice polymer simulations. They are believed to produce reasonably realistic dynamics (see references 28, 29, 30, 31 for details). For

thermodynamics calculations, it is not necessary to use a move set with this property, and other move sets have been used.^{21, 23} There are however, two potential problems with realistic dynamic move sets: ergodicity and glassy behavior. If one is interested only in kinetics, then these are not really problems but rather properties of the model. For thermodynamic calculations, inaccessibility is not a problem either, since we can consider the definition of the model to include only the states accessible by the move set specified (hence it will be by definition ergodic). Therefore, as long as the minimum energy cube state is accessible from an unfolded chain, there will be no problems.

The glass transition presents a more difficult problem for thermodynamic calculations. At low temperatures, the dynamics of the system slow down substantially. In particular, the correlation times become quite large and it takes longer to explore conformational space. This gives rise to two errors in the Monte Carlo calculations. First, it takes a long time for the system to relax, making it difficult to get the system into thermal equilibrium. This contributes a systematic error to the results and it can give rise to the hysteresis effect seen in the previous studies.^{21, 32} Second, because of the long autocorrelation times subsequent samples are no longer statistically independent of each other. This has the effect of increasing the variance of any observable (and the corresponding statistical error). The actual variance is given by:

$$\sigma_{\text{actual}}^2 = (1 + 2\frac{\tau_{\text{ac}}}{\tau_{\text{samp}}})\sigma^2 \quad (3)$$

where σ^2 is the usual variance calculated from the samples. τ_{ac} is the integrated autocorrelation time and τ_{samp} is the number of time steps between samples (both measured in units of Monte Carlo steps).^{33, 34} As τ_{ac} increases, longer simulations are necessary to get statistically reasonable results. That is, in a simulation of N steps there will be N/τ_{ac} “effectively independent samples.”³⁴ At low temperatures the time required to obtain enough independent samples becomes enormous. One solution is to use a different move set, such as the Rosenbluth chain growth algorithm.^{22, 21, 23} The auto-correlation time for this move set does not increase as rapidly, allowing simulations at lower temperatures. Our solution instead is to run the simulations well above the glass transition temperature, and then to use the histogram method to extrapolate to lower temperatures.

B Techniques for calculating thermodynamics quantities

For short enough chains (usually in two-dimensions) it is possible to enumerate all lattice conformations and thereby calculate the partition function for the system along with any other quantity of interest.¹³ For the three-dimensional 27 monomer chain, it is not practical³⁵ to enumerate all conformations but it is possible to enumerate all of the maximally compact (cube) conformations. One could then approximate the partition function by just summing over the cube states. Previous studies have used this method to calculate thermodynamics quantities of this system. It was hoped that at low temperatures this approximation might be reasonable. We show later that, although it can give rough qualitative results, using only the cube states leads to appreciable errors.

Since exact enumeration is impossible, Monte Carlo sampling is used for calculating thermodynamic quantities. The usual technique runs the simulation at a given temperature, collecting samples to determine thermal averages. The process is repeated for several temperatures to get the averages as a function of temperature. There are several drawbacks to the standard Monte Carlo procedure. Calculating extensive variables like the free-energy or entropy is difficult. Also, if one wants to find peaks or zeros of a given quantity (like the specific heat peak, to identify the transition temperature), one must scan over a range of temperatures to locate the critical value.

It is possible to extract more information from a single Monte Carlo run than just the thermal averages at the temperature the simulation was performed. The technique is called the histogram method or density of states method. It has a long history and it has been recently rediscovered by a variety of authors.^{25, 26, 36, 37, 38, 39} The actual Monte Carlo sampling algorithm itself is unchanged. But instead of just calculating thermal averages, one keeps track of the number of times a specific energy is encountered in the simulation; i.e., an energy histogram is calculated. This histogram, $h(E, T)$, measures the probability of energy E occurring at temperature T . It is equal to the thermal average of the density of states:

$$h(E, T') = \frac{n(E)e^{-E/T'}}{Z(T')}, \quad (4)$$

where $Z(T')$ is the partition function at temperature T' is

$$Z(T') = \sum_E n(E)e^{-E/T'}, \quad (5)$$

and $n(E)$ is the density of states for energy E (the number of conformations with energy E). The Boltzmann factor k_b has been set equal to 1 and T' is the temperature of the simulation. One now has the density of states up to a multiplicative factor:

$$n(E) = h(E, T')e^{E/T'}Z(T'), \quad (6)$$

where $Z(T')$ is the unknown multiplicative constant. For intensive quantities, thermal averages are calculated using:

$$\begin{aligned} \langle \mathcal{O} \rangle (T) &= \frac{\sum_E \mathcal{O}(E)n(E)e^{-E/T}}{\sum_E n(E)e^{-E/T}} \\ &= \frac{\sum_E \mathcal{O}(E)h(E, T')e^{-E/T+E/T'}}{\sum_E h(E, T')e^{-E/T+E/T'}}. \end{aligned} \quad (7)$$

Note, $Z(T')$ cancels out of the above expression.

If one is interested in calculating extensive quantities like the free energy or the entropy, it becomes necessary to determine the constant $Z(T')$.⁴⁰ For our system, it is possible to calculate this constant and therefore obtain the density of states. To determine this constant, all we need is the multiplicity of any energy state. For example, the sequences we study have a non-degenerate ground state. This means $n(E_{gs}) = 1$, where E_{gs} is the energy of the lowest energy cube. $Z(T')$ can then be determined and the free energy is then calculated using $F = -T \log Z$ and equation 5.

There is a limit to the temperature range over which equation 7 is valid. For temperatures too far from the simulation temperature, the errors in the density of states calculated from equation 6 become significant. At any given temperature, the system is only sampling a given region of phase space.⁴¹ For example, figure 2 shows energy histograms at a high and a low temperatures. For the high T simulations, the ground state is never probed, and likewise for the low T some high energy states are never reached. Consequently, the density of states will be incorrect for regions not sampled properly (in fact it equals zero for regions that are never sampled). This limits the temperature range we can extrapolate from any simulation. One needs to monitor the errors in the density of states. A solution to this problem is the multiple histogram method.²⁶ The idea is to use several different simulations and patch the histograms together. Although there are some subtleties to this technique, it can be powerful.

For the 27 monomer long polymer used here, a single histogram gives adequate results over the range of temperatures of interest. The reason is that the width of the energy histograms in general scale as

$1/\sqrt{N}$, where N is the system size. As we shall show shortly, the system is small enough to insure that the histograms are broad and a large region of phase space is sampled at any given temperature.

III RESULTS AND DISCUSSION

Several Monte Carlo runs were performed over a range of temperatures. Six sequences were used all with a fixed ratio of monomer types (14 to 13). Table 1 lists the sequences and the energy of their native states. To get some idea of what a typical (i.e. randomly chosen) sequence is and how it compares to the sequences used in this study, we generated over 10,000 random sequences (with a 14:13 ratio of monomer types). Approximately 1,000 sequences had unique ground states. Figure 3 shows a histogram of the ground state energies for these sequences. The distribution is roughly gaussian. The most probable energy is approximately -76. One sequence examined (sequence 013) has a typical ground state energy for random sequences. We did not generate any of the minimum energy (-84) sequences at random. The two that we used were both designed: one using a Monte Carlo algorithm⁴² and the other by mutating a -82 energy sequence. The thermodynamic averages of several quantities (average energy, contacts, native contacts, specific heat, etc.) were calculated at

Run	Sequence	E_{\min}
002	ABABBBBABBABABAABAAAAAAB	-84
004	AABAABAABBABAABABBABABBB	-84
005	AABAABAABBABAABBBABABBB	-82
006	AABABBABAABBAAAABABAABBB	-80
007	ABBABBAABABAABABABBBBABA	-80
013	ABBBABBAABBBAAABBABAABABA	-76

Table 1: The various sequences used in this paper. The last four (005, 006, 007, 013) were generated at random. Sequence 002 was optimized by Shakhnovich (Ref. 42). Sequence 004 is a single monomer mutation of 005 ($B_{13} \rightarrow A$). Both 002 and 004 have the lowest energies possible for the potential used and have native states that are completely unfrustrated. E_{\min} is the energy of the native states. These same six sequences were studied in our previous work (Ref. 9) which examined the kinetics of folding.

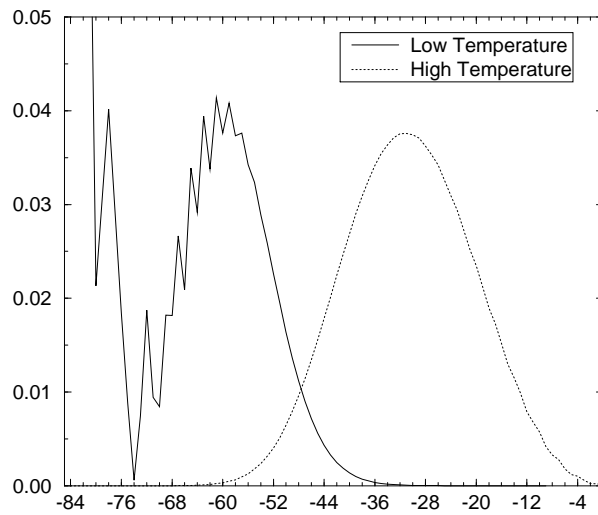


Figure 2: Energy histograms taken at high ($T = 3.15$) and low ($T = 1.41$) temperatures. Note that for each histogram there are regions of energy that are not sampled at all. In particular at high temperatures the ground state is not probed while at low temperatures the high energy (unfolded) conformations are not probed.

each of the simulation temperatures. In addition, histograms of the number of like versus unlike contacts (N_l and N_u) were calculated. We chose to histogram these variables instead of the energy directly because these histograms can be used to extrapolate not only other temperatures but other parameter values (E_l and E_u).

Figure 4 shows the folding time and collapse times as a function of the inverse temperature. The two different collapse times are the time to find the first cube (i.e., a maximally compact state) and the time to form the first 25 (out of 28) contacts. For high temperatures, the collapse times are sequence independent (*self-averaging*). The folding times are sequence dependent. Similarly, the collapse times below the glass transition are also sequence dependent. The kinetic glass transition temperature was defined in our previous work⁹ as the temperature at which the folding time is half way between its minimum and maximum value (the maximum being determined by the time limit on the simulation and chosen to be much longer than the fastest folding time). Both the folding and collapse time show non-Arrhenius behavior at high temperatures.

A Histograms: First vs. second order transitions

Before using the histograms to calculate the density of states, we examined them to determine how much

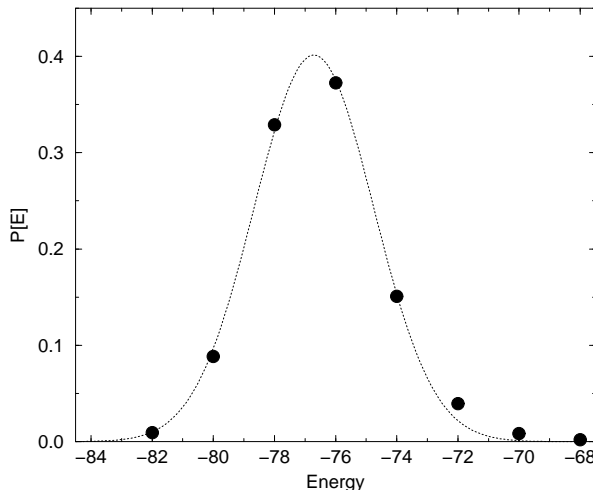


Figure 3: Ground state energy histogram for non-degenerate sequences. 13,563 sequences with a fix ratio of monomer types (14:13) were generated at random. The energy and multiplicity of the minimum energy cube was determined from exhaustive enumeration of the cube conformations. 1,061 sequences (7.8%) were found to have unique ground states. The histogram of ground state energies from these sequences is plotted (solid circles). The dotted line is a least squares fit of a gaussian to the data. Note, we did not find any minimal energy (-84) sequences in our random sample. The total number of possible sequences is $\binom{27}{14} = 20,058,300$.

of phase space is sampled at different temperatures. This (as mentioned above) determines how far we can extrapolate from the simulation temperature using the histogram technique. Figure 5 shows the energy histogram for sequence 002 for several temperatures. Because of the small size of our system, they are all rather broad, with widths of roughly 30 energy units. Examining the behavior of the curves as a function of temperature, we see the both first and second order-like behavior of the system. At high temperatures (between 5 and 2, see fig. 5a) a single energy peak moves steadily to lower values. This is what would be expected from a second order-like transition. At lower temperatures (fig. 5b) the plots now have a bimodal distribution and as the temperature is decreased there is a shift from one peak to the other. This is characteristic of a first order-like transition. If we examine the histograms as a function of the number of contacts, the same behavior is seen (fig. 6). At high temperatures the plots are unimodal and shift to larger number of contacts (higher compactness) as the temperature is lowered. This continues un-

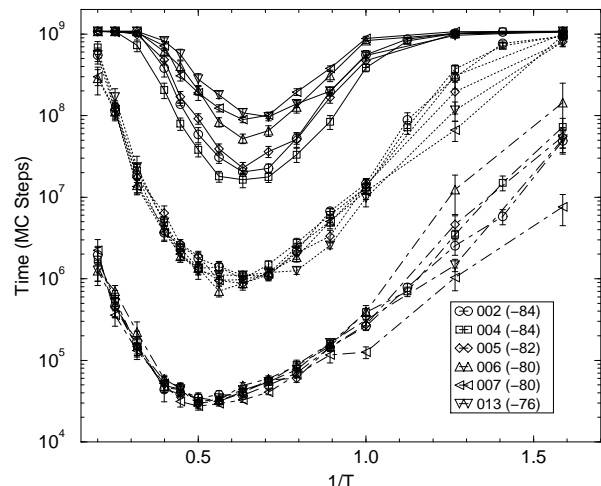


Figure 4: Folding and collapse times versus inverse temperature. Time is in Monte Carlo steps. The solid lines represent the mean folding time. The middle dotted lines represent the mean compaction time to any cube. The bottom lines represent the mean compaction time to a partially compact conformation with 25 (out of 28) contacts. Error bars are the standard deviation of the mean. Note, simulations were run for a set amount of time τ_{\max} . For high and low temperatures some runs were not able to find the folded (or compact) state in this time. In these cases τ_{\max} was averaged in, so the times shown are lower bounds to the actual mean first-passage times.

til the maximum reaches roughly 20 contacts around $T = 2$. At lower temperatures this peak remains fixed at about 20 contacts and another peak forms at 28 contacts. Because this peak at 28 contacts occurs at low temperatures and when there is a peak at -84 in the energy histograms, we expect that it is due to occupation of the native state and the few other low energy cubes. As the temperature is decreased there is a shift in population between the two peaks. This is consistent with the idea that there are two thermodynamic transitions: a collapse to compact structures and a folding transition to the native state. The collapse transition occurs at a higher temperature and is second order-like. The folding transition is first order-like.

Since the histograms are broad enough we used the single histogram technique in the subsequent calculations. Because we are interested mainly in the properties of the ground state, we chose a temperature which is low enough for the ground state to be sufficiently populated and yet high enough so that we sample as much of the conformation space as pos-

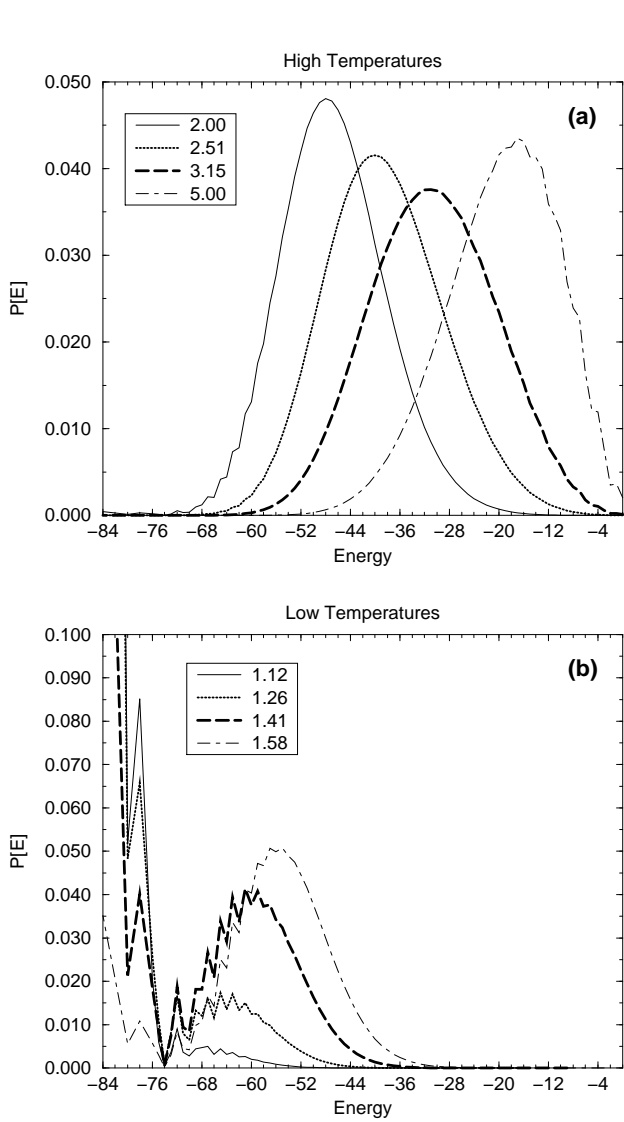


Figure 5: Histograms of energy for several temperatures. The sequence is number 002. For high temperatures (a) the plots have one peak which moves to lower energies as the temperature decreases. For low temperatures (b) the plots are bimodal.

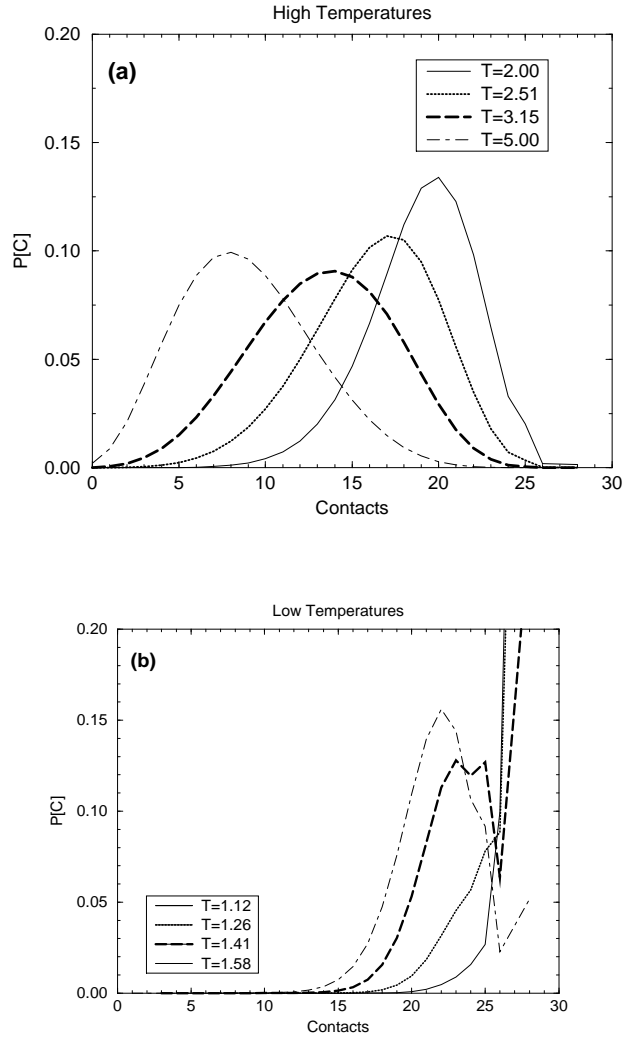


Figure 6: Histograms of contacts for several temperatures, again for sequence 002. The behavior of the plots is similar to that of the energy histograms (see fig. 5). As the temperature is lowered a single peak moves from a low to a high number of contacts until it reaches roughly 20 (a). At this point a second peak forms at 28 contacts and we see a first order-like transition between the two (b).

sible. At a temperature of 1.58 there is a sizeable peak at the ground state and substantial sampling of the higher energy conformations. Kinetically it turns out that $T = 1.58$ the chains fold most rapidly (i.e., the mean first-passage time to the folded state is smallest). So we expect at this temperature we are moving most rapidly through the compact conformations. Since this temperature is far enough away from the kinetic glass temperature (which was previously measured to be approximately 1 for this system) we do not have to worry about the problem of long relaxation times which would make it difficult to equilibrate and would require a long sampling time to reduce statistical errors. We calculated the energy autocorrelation function:

$$C_E(t) = \frac{\langle E_\tau E_{\tau+t} \rangle - \langle E \rangle^2}{\langle E^2 \rangle - \langle E \rangle^2} \quad (8)$$

where E_τ is the energy of the system at time step τ . At long times this function should have the following form:

$$C_E(t) \sim e^{-t/\tau_{ac}} \quad (9)$$

where τ_{ac} is the autocorrelation time.³⁴ At the temperature $T = 1.58$ we get an autocorrelation time of roughly 500,000 Monte Carlo steps. For all our thermodynamic simulations we equilibrated our system for $20\tau_{ac}$ and ran for 1.08×10^9 steps (2000 times τ_{ac} which gives roughly 2000 independent samples).

B Density of states

Using the histograms from the Monte Carlo simulations and equation 6 the density of states for the various sequences is calculated. Figure 7 shows the densities for three sequences with low, medium and high values for E_{\min} (002, 006, 013). For comparison the cube spectrum, determined by exact enumeration, has also been plotted. At low energies the the density of states is different for each sequences. In particular, sequence 002 has more low energy conformations that are not cubes as compared to 006 and 013. All three sequences have a notch in their density, but the gap between the notch and the folded state is larger for sequence 002 than for the others.

At energies below -60 the densities of states for the three sequences are roughly the same. This part of the spectrum is *self-averaging* as expected since it should depend on only the ratio of monomer types. At very high energy there is considerable scatter in the plots. This is due to the poor sampling of this area of conformational space. In particular, the

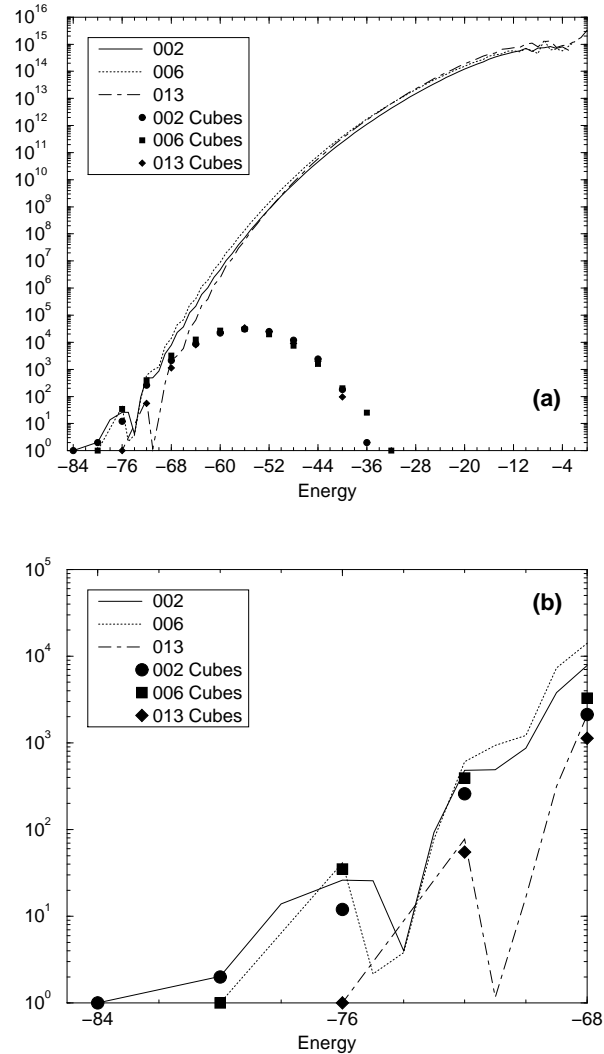


Figure 7: Density of states versus energy calculated using the Monte Carlo histogram technique. Three different sequences are shown (002, 006, 013) with different ground state energies. The first plot (a) is the full density of states. The lines are from the Monte Carlo calculation. The points show the density of states for just the cube conformations (determined by exact enumeration). The second plot (b) is a blow-up showing the low energy region of the first. At high energies the densities of states are sequence independent while at low energies they are strongly sequence dependent.

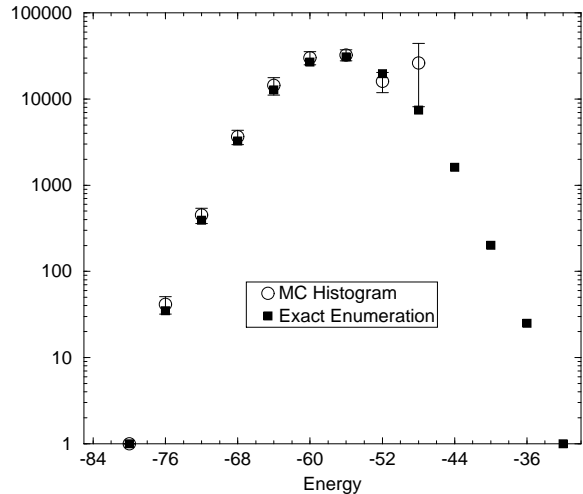


Figure 8: Comparison of the cube spectrum from exact enumeration and from the Monte Carlo histogram calculation. Error bars are the standard error of the mean from several Monte Carlo runs. The temperature of the simulations was 1.58. At this temperature the average energy is -55.5 and the percent of population in the ground state is 0.2%.

curves in figure 7 for sequence 002 and 006 do not even extend to zero energy, indicating that these conformations are not sampled at all. However, we expect that for low temperature thermodynamic calculations this will not pose problems.

As a simple check of the accuracy of the Monte Carlo histogram technique in this system, we compare the exact cube spectrum (from enumeration of all cubes) to the cube spectrum calculated from the histogram data. Remember that there is an unknown normalization factor, which we determined by setting the density of states for the lowest energy cube equal to 1. Figure 8 shows the comparisons. For cubes up to an energy of -52 there is excellent agreement between the histogram calculation and the exact answer. At high energies we see the same sampling problem; cubes with energy greater than -50 are not sampled at all, since they make up a negligible fraction of the conformations at these energies. However, for low temperature calculations the errors should be negligible.

C Computing thermodynamic quantities

Figure 9 is a plot of the average energy as a function of temperature for the same three sequences (002, 006 and 013) whose densities of states are shown in

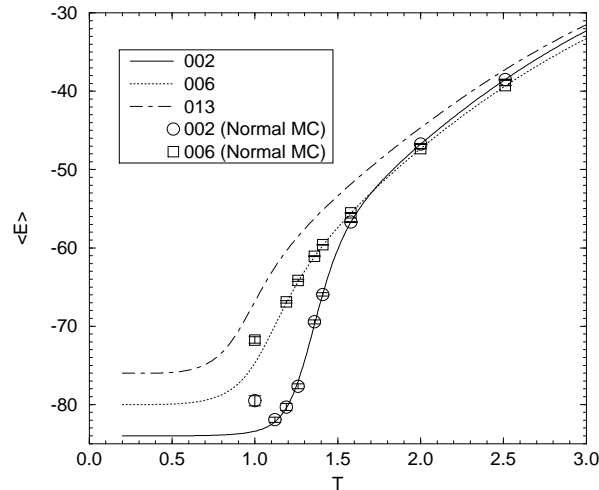


Figure 9: Average energy versus temperature for three different sequences (002, 006 and 013). The lines are calculated using the histogram technique from simulations at $T = 1.58$; the points are from normal Monte Carlo simulations (i.e., they were calculated from the usual averaging technique at several different temperatures). For most temperatures there is excellent agreement between the two. As we approach the glass temperature the normal Monte Carlo technique starts to deviate due to the divergence of the relaxation (equilibration) time of the system.

figure 7. At high temperatures ($T > 2.5$) all their sequences have the roughly the same average energy. At lower temperatures the sequences are no longer self-averaging. The two sequences with the higher energy folded states (006 and 013) have a fairly broad transition while the low energy sequences (002) have a comparatively sharper transition. A similar result is seen in the specific heat, which is plotted in figure 10. Sequence 002 has a much sharper and higher specific heat peak which occurs at a higher temperature. The other sequences have broader smaller peaks. The peak in the specific heat occurs at temperatures slightly higher than the folding temperature (see tab. 2) and indicates the transition from the unfolded chain to the collapsed state rather than the transition to the native state. At high temperatures the specific heat is sequence independent.

Also included in figures 9 and 10 are data points calculated using the standard Monte Carlo averaging technique for comparison. There is excellent agreement between the histogram curves and the points up until the kinetic glass temperature (which is at $T \approx 1$ for these sequences). At the glass temperature the usual Monte Carlo technique has a problem with

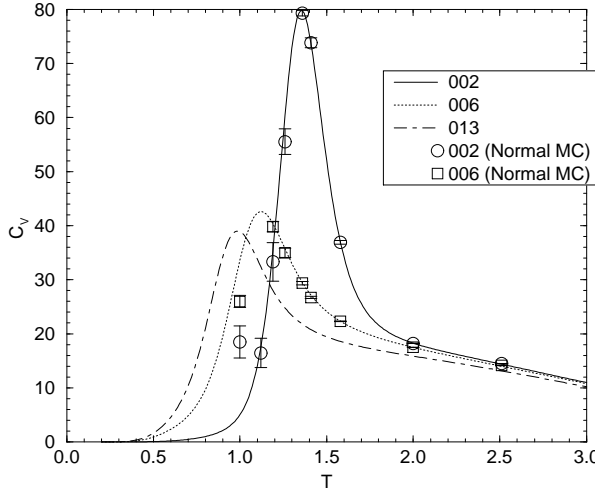


Figure 10: Specific heat versus temperature for sequences 002, 006 and 013. The lines are calculated using the histogram technique from simulations at $T = 1.58$; the points are from normal Monte Carlo simulations (i.e., they were calculated from the usual averaging technique at several temperatures). At the kinetic glass temperature ($T = 1$) there is substantial error in the normal Monte Carlo result.

the increasing autocorrelation time (all simulations were equilibrated and sampled for the same amount of time). The histogram method, however, allows us to probe beyond the glass temperature since the low energy states can be sampled accurately at higher temperatures (see fig. 8).

One useful feature of the histogram technique is the ability to determine extrema and zeros of thermodynamic functions. For example, the folding temperature T_f is the temperature at which the population of the native state equals one half:

$$P_{\text{nat}}(T_f) = \frac{e^{-E_{\text{nat}}/T_f}}{Z} = \frac{1}{2}. \quad (10)$$

Once the density of states has been determined, one can numerically solve for T_f using any standard root-finding algorithm.⁴³ Figure 11 plots $P_{\text{nat}}(T)$ for the three sequences along with the folding temperatures. Also shown is a plot of the probability of being semi-compact (which we define as structures have 20 or more contacts):

$$P_{c_{20}}(T) = \frac{\sum_E \sum_{C \geq 20} n(E, C) e^{-E/T}}{Z}, \quad (11)$$

where $n(E, C)$ is the density of states as a function of energy and contacts. Note that in order to compute this quantity we need to keep track of histograms as

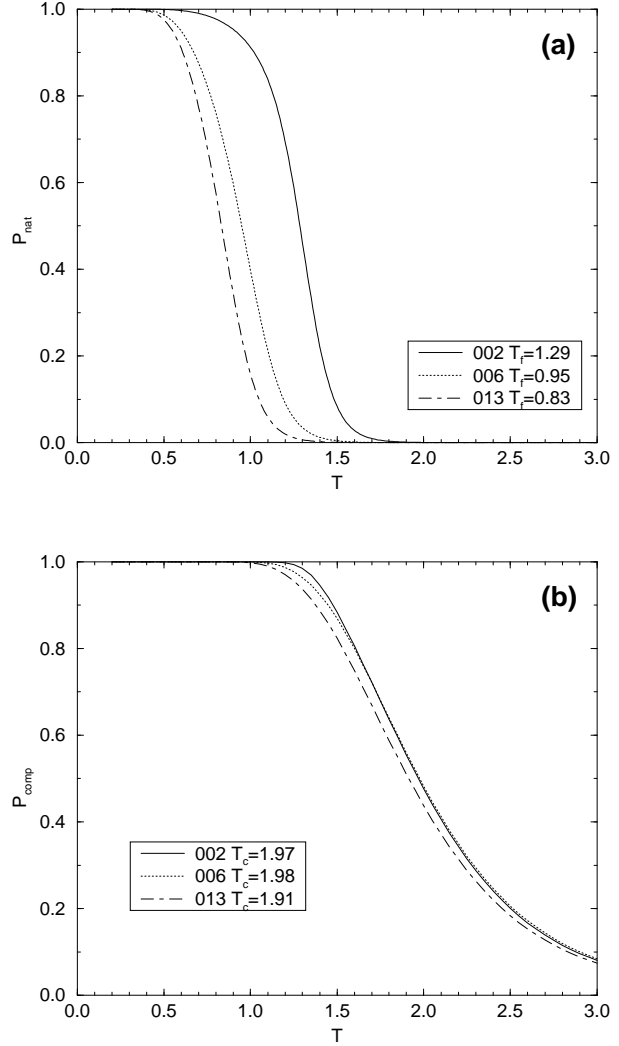


Figure 11: Folding and collapse transitions for sequences 002, 006 and 013. Figure (a) is a plot of the probability to be in the native state (P_{nat}) versus temperature, while figure (b) plots the probability to be compact (20 out of 28 contacts, $P_{c_{20}}$). The folding temperature is defined as the temperature at which $P_{\text{nat}} = \frac{1}{2}$. The collapse temperature is defined similarly. The folding temperature is a sequence-dependent quantity while the collapse temperature is roughly sequence-independent (self-averaging). We expect the collapse transition to depend on the ratio of monomer types (i.e., the over-all drive to compactness) and therefore it should not depend on the specific sequence.

Run	Full DOS	Cubes	Percent Error
002	1.29(2)	1.763	37.2%
004	1.26(1)	1.695	34.1%
005	1.15(2)	1.429	24.2%
006	0.94(6)	1.049	11.5%
013	0.83(5)	0.935	12.6%

Table 2: Comparison of the folding temperature T_f calculated using the full density of states (from the histogram method) and just the cube states (from exact enumeration). Numbers in parentheses are the uncertainty in the last digit. The last column is the percent error of the cube-only calculation.

a function of energy and contacts. Histograms of just the energy would not have allowed us to sort out the compact states from the non-compact ones. Similar to T_f the compaction temperature T_c occurs when the probability of being semi-compact (20 contacts) equals one half. Figure 11 shows the $P_{c_{20}}$ curves along with the values for T_c . We chose 20 contacts because that was the point at which the histograms (see fig. 6) changed from their second order to first order-like behavior. Therefore, we expect that measuring this quantity will probe the first transition from random coil to globule (semi-compact) states.

As expected the folding temperature (T_f) is sequence dependent. Also, the transition curves for folding are much sharper than they for collapse. The lower the energy of the ground state the higher the folding temperature for that sequence. In contrast, the compaction temperature (T_c) is almost sequence independent (it varies by only 4% versus a 43% difference for T_f). One would expect the compaction temperature to be self-averaging since it should depend on the average composition of the sequence (which is the same for all sequences used in this work). At the compaction temperature the native state occupation (P_{nat}) is very small. This is consistent with the previous observation from the histograms (see figs. 5 and 6). There are two separate thermodynamic transition: collapse from a random coil and then folding to the native state.

It is clear from figure 7 that using just the cubes to calculate thermodynamics can lead to potentially large errors. Table 2 compares the folding temperature calculated using the full density of states with the temperature calculated solely on the basis of cube states. The cube results consistently over-estimate the folding temperature. This is not surprising since many low energy non-cube states are being neglected.

These states will reduce the stability of the native state. The cube approximation is better for the non-folding high energy sequences than for the low energy sequences. Consequently, it fails more seriously for the sequence we are most interested in, namely the good folding sequences.

D Combining kinetics and thermodynamics—unfolding time

Much of the work (both experimental and theoretical) on protein folding deals with the forward process (unfolded to folded). However, studying the reverse process, the unfolding of nascent proteins, may not only provide a wealth of information, but may also be a great deal easier. In unfolding simulations, the initial condition is well-defined (the folded state) and by varying the various parameters it is fairly easy to induce unfolding. There have been several works examining unfolding using detailed molecular dynamics simulations.^{44,45}

Using the data previously calculated, we can compute an unfolding time for our lattice chains. We first make the two-state assumption, namely that there is an unfolded state (U) that is in thermal equilibrium with the folded state (F):

$$F \rightleftharpoons U. \quad (12)$$

We can then calculate an unfolding time (τ_u) as follows:

$$\tau_u(T) = \frac{[F]}{[U]} \tau_f(T) \quad (13)$$

where $[U]$, $[F]$ are the populations of the unfolded and folded state respectively and $\tau_f(T)$ is the folding time as a function of temperature. The ratio $[F] / [U]$ is given by $P_{\text{nat}}(T) / (1 - P_{\text{nat}}(T))$, using $P_{\text{nat}}(T)$ defined by eq. 10. Figure 12 shows a plot of the unfolding time versus $1/T$ for several sequences. Unlike the folding time (fig. 4), the unfolding time has a much simpler behavior. For temperatures above the kinetic glass temperature (T_g), the unfolding times vary almost linearly with $1/T$ and have slightly different slopes for the various sequences. The slopes are roughly proportional to T_f ; sequences 004 and 002 have the steepest slopes and 013 has the shallowest. In contrast to the folding time, which shows clear non-Arrhenius behavior over this temperature range, the unfolding time is nearly Arrhenius. We expect due to the large enthalpic barrier that entropic effects are less noticeable in unfolding than folding. At low temperatures the unfolding time rolls off due to the cutoff in the simulation time (this is the same

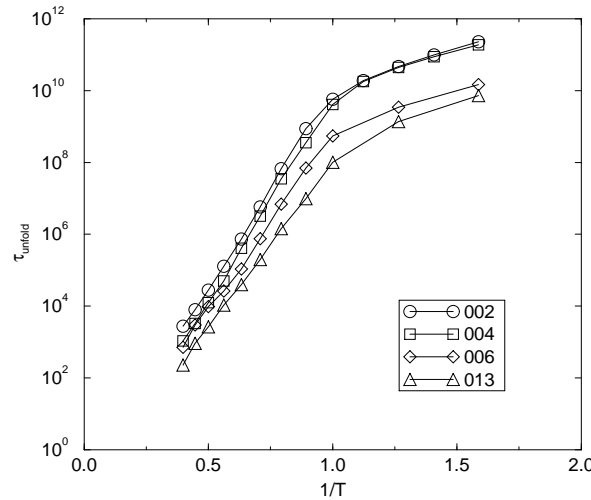


Figure 12: Unfolding times versus $1/T$ for several sequences. The time is plotted on a log scale. The linear relationship between time and $1/T$ for temperatures greater than T_g is much simpler than the behavior of the folding time.

roll-off seen in the folding time at low temperatures; see fig. 4).

E Exploring parameter space

All the results so far have been for simulations with contact energies $E_{\text{avg}} = -2$ and $\Delta = 2$ ($E_l = -3$ and $E_u = -1$). These values were chosen to insure that the ground state (native state) would be a cube. For sequences like 002 and 004 there exists a cube (out of the 103,346 possibilities) that has no weak contacts (contacts between different monomer types). This cube will be the ground state as long as $E_l = (E_{\text{avg}} - \Delta/2) < 0$, irrespective of what E_u is (i.e., E_u can be greater than zero). We call these sequences *unfrustrated*. All of the other sequences have at least one weak contact between unlike monomers even in their lowest energy cube (see fig. 13). These are *frustrated* sequences. For frustrated sequences, it is not clear that the minimum-energy cube will be the minimum-energy conformation. There may be some non-cube conformation with fewer total contacts but more good contacts than the cube conformation. For sequence 005, which has 27 good contacts in its minimum cube conformation, and 006 and 007, which have 26 good contacts, there are no other conformations that have more good contacts. Consequently, the cube conformations will be the ground states as long as $E_u = (E_{\text{avg}} + \Delta/2) < 0$.⁴⁶ For sequence 013,

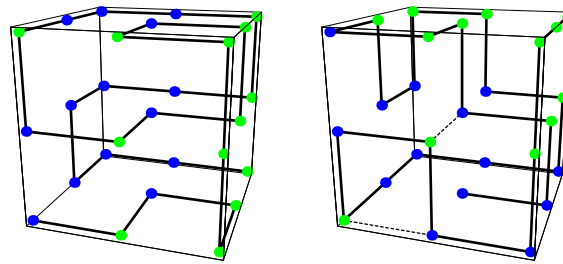


Figure 13: The native conformations of sequence 002 (left) and 006 (right). Note that 006 has 2 “weak” contacts (indicated in the figure with dotted lines) in its lowest energy state.

which has 24 good contacts in its minimum-energy cube, it is possible that there is some non-cube conformation with more than 24 good contacts. We can not exhaustively enumerate all the non-cube conformations but we can state empirically that no conformation with a lower energy was found in any of the Monte Carlo runs (see note 46).

We now explore how the model behaves as we vary the potential parameters. Specifically, how do the various kinetic and thermodynamic properties depend on these parameters? Sequence 002 was examined in detail. As mentioned, this sequence has an unfrustrated cube conformation (see fig 13). This cube will be the ground state whenever $E_l < 0$. If E_l is greater than zero then the minimum energy conformation is the completely unfolded chain with no contacts. This clearly would not represent a protein under folding conditions; thus we ignore this region of parameter space. Several simulations with various values⁴⁷ of E_{avg}/Δ ranging from 0 to approximately 2.5 were run.⁴⁸ Figure 14 shows a plot of the folding and compaction times versus E_{avg}/Δ . The times plotted in these figures are taken from the temperature with the fastest time (i.e., the minimum point in figure 4) for each value of E_{avg}/Δ . As the absolute value of E_{avg}/Δ is decreased from 2.5 to 0, both compaction times (the time to form 25 and 28 contacts) increase, although the change is small. This is expected since the drive to form contacts decreases as $|E_{\text{avg}}/\Delta|$ is reduced. For the folding time there is an opposite and more dramatic effect. Decreasing $|E_{\text{avg}}/\Delta|$ decreases the folding time (τ_f), almost two orders of magnitude. Also, at $E_{\text{avg}} = 0$, τ_f almost equals τ_{28} (the time to make 28 contacts). What is happening is that as $|E_{\text{avg}}/\Delta|$ decreases, we are destabilizing non-native cubes relative to the native state. At large $|E_{\text{avg}}/\Delta|$, these low energy non-native cubes behave as traps slowing down the fold-

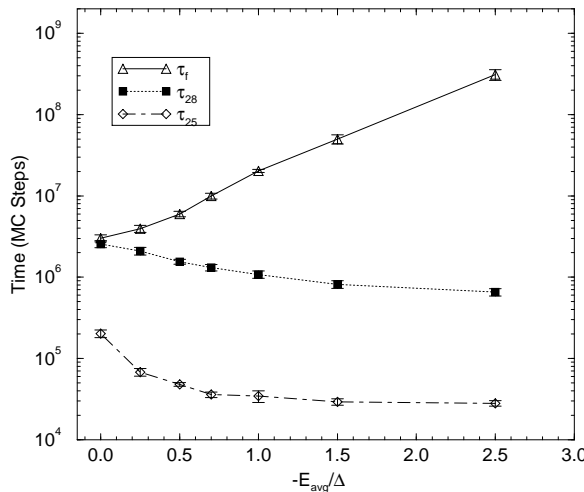


Figure 14: The minimum folding time and the compaction times plotted as a function of E_{avg}/Δ for sequence 002. The line with the triangles is the mean folding time (i.e., the time to find the native state). The squares are the mean time to find the first cube state (not necessarily the native state) and the diamonds are the mean time to find a conformation with 25 contacts. For each of these times, there is a minimum point in the point of time vs temperature (see fig. 4). It is that minimum (fastest) time that is plotted here for each value of E_{avg}/Δ .

ing rate. Reducing $|E_{\text{avg}}/\Delta|$ increases their energy relative to the native cube eliminating them as traps. This in turn increases the folding rate. Alternatively, as $E_{\text{avg}}/\Delta \rightarrow 0$, E_u increases until it becomes positive. At this point making weak (incorrect) contacts is unfavored relative to breaking them. This keeps the chain from forming these weak, incorrect contacts which would trap it in states different from the native state. The chain is more effectively funneled into the native conformation; i.e., the first cube made is almost always the native one. By varying E_{avg}/Δ we can control the time-scale separation between folding and collapse to maximally compact states.

Next, we examined how the folding temperature (T_f) and the kinetic glass temperature (T_g) varied as a function of E_{avg}/Δ . In particular, for which values of E_{avg}/Δ is T_f greater than T_g ? For these values of E_{avg}/Δ , the chain will fold before the native state becomes inaccessible. The histogram method is used to calculate T_f for various values of E_{avg}/Δ . The technique is the same as the one used to extrapolate to different temperatures. In this case one needs histograms as a function of good and weak contacts (which can be calculated from the energy

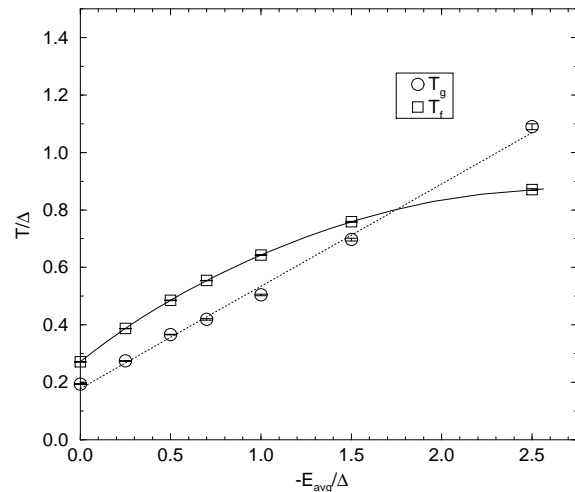


Figure 15: A plot of the folding temperature (T_f) and the kinetic glass temperature (T_g) as a function of the average drive to compactness (E_{avg}). Both the temperatures and the energies have been scaled by Δ . The dotted line is a linear fit of the glass temperatures. The solid line is not a fit to the T_f points but was calculated explicitly via the histogram technique. For values of E_{avg}/Δ approximately less than 1.7 $T_f > T_g$ so the chains will fold before hitting the glass transition. For E_{avg}/Δ greater than 1.7 the glass transition occurs before folding so the chains do not reach their ground state within the simulation time.

contact histograms previously used). To calculate T_g we must run simulations at various values of E_{avg}/Δ since there is no way to extrapolate as in the case of T_f . The two temperatures (T_f and T_g) are plotted for sequence 002 in figure 15. Note that we plot the temperature normalized by Δ (i.e., in units of Δ) just as we plot E_{avg} normalized by Δ .⁴⁸ The glass temperature varies almost linearly with E_{avg}/Δ . Previous work on glass transitions in heteropolymers have shown that the transition occurs after the collapse of the system.^{49,50} In fact it was shown that the polymer needs to collapse in order to have a glass transition. This is consistent with the behavior we see: as $|E_{\text{avg}}/\Delta|$ increase so does the collapse temperature (T_c). In fact as we will see shortly $T_c > T_g$ for all values of E_{avg}/Δ . As $|E_{\text{avg}}/\Delta|$ increases, the depth of the local minima increases relative to the unfolded state. It becomes harder to escape from local traps so the chain “freezes” at higher temperatures.

The folding temperature also increases as the absolute value of E_{avg}/Δ increases but reaches a limiting value. This behavior of T_f with E_{avg} is easy

to understand. As $|E_{\text{avg}}/\Delta|$ is increased, the stability gap becomes larger; hence T_f increases. However, it eventually asymptotes to a limiting value of approximately 0.87. This limiting value turns out to be precisely the folding temperature that would be calculated using just the cube conformations. In table 2 we see that for sequence 002 $T_f = 1.763$ for the cube-only calculation. In calculation $\Delta = 2$ so we need to divide the temperature by 2, giving 0.88. The reason T_f approaches the cube-only value is that as $|E_{\text{avg}}/\Delta|$ increases the cube states decrease in energy more than the non-cube states since they have more contacts. Eventually, at low enough E_{avg}/Δ all the low energy states are just cubes. It is the low energy states that determine T_f . Once T_f reaches this limit, it is unchanged by further changes to E_{avg}/Δ since the relative energy between the various cube states is determined by Δ which we are holding constant at 1.

Looking at both the T_f and T_g lines we see there is a key point at which T_g becomes greater than T_f . At $E_{\text{avg}}/\Delta \approx 1.7$ the chains become glassy before they become thermodynamically stable; consequently, they will not be able to fold. For E_{avg}/Δ greater than 1.7, $T_g > T_f$. The chain is trapped in local minimum and will not find the native state within the simulation time. When E_{avg}/Δ is less than 1.7 $T_g < T_f$, so the chains fold to the native state and will be thermodynamically stable before the dynamics slow down. By including the results for the collapse transition temperature (the temperature at which half the chains have at least 20 contacts) a qualitative phase diagram can be drawn (see fig. 16). There are four regions: random coil, collapsed globule, folded and collapsed frozen state. The phase diagram is very similar to other lattice models and theoretical calculations of heteropolymers.^{51,52} The vertical dotted line represents the transition from the glassy to folded phase. To the right of it (i.e. large $|E_{\text{avg}}/\Delta|$) $T_f/T_g < 1$ and to the left of the line (small $|E_{\text{avg}}/\Delta|$) $T_f/T_g > 1$. As $|E_{\text{avg}}/\Delta|$ is decreased the folding and collapse curves converge. This is the same behavior observed in the kinetic data (see fig 14). As E_{avg}/Δ approaches zero, E_u becomes positive. Collapsed states with weak contacts will be unfavored relative to states with no contacts. This drives the polymer to form only correct (good) contacts, so the chains will collapse almost directly to the correctly folded state. Another way to understand this is that non-native cube conformations are unfavored as E_u increases. At $E_{\text{avg}}/\Delta = 0$ roughly half of the cubes for sequence 002 will have positive energies. This removes them as possible kinetic traps. For all values of E_{avg}/Δ , the collapse temperature is greater

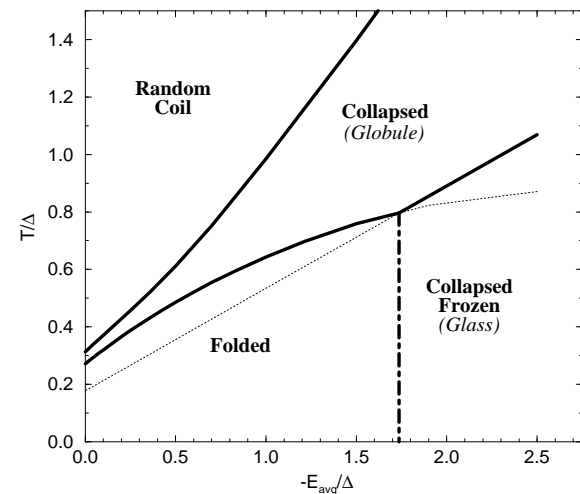


Figure 16: Phase diagram for sequence 002. There are four regions: random coil, collapsed globule, collapsed frozen, and folded. The solid line between the random coils and the collapsed globule state is the collapse transition, the temperature at which half the chains have 20 contacts. The second solid line is equal to either T_f or T_g , whichever is greater at that value of E_{avg}/Δ . The dotted line equals the lesser of T_g or T_f . The vertical dash-dotted line shows the transition from the folding region (where $T_f > T_g$) to the frozen region. It occurs at $E_{\text{avg}}/\Delta \approx -1.7$.

than not only the folding, but also the glass, temperature. Previous heteropolymer mean-field calculations⁴⁹ show that T_g must be less than T_θ , the collapse temperature, consistent with what we find here. Perhaps most interestingly, we see that by modulating a single parameter in our model we obtain a range of qualitatively different folding behaviors. Recently, work has been done on the classification and examination of the various possible folding regimes with a comparison to experimental data.⁷

IV CONCLUSIONS

We have continued our comprehensive analysis of the 27 monomer cube lattice heteropolymer. The Monte Carlo histogram method proved extremely useful, allowing us to determine the density of states for this system and then to calculate a broad range of thermodynamic quantities. In particular, the method overcame the problem of dynamical slowing down at low temperatures. Like many other heteropolymer studies (both analytical and numerical) we find two different transitions: a collapse transition with a roughly sequence-independent collapse temperature and a folding (to the native state) transition with

a sequence-dependent folding temperature. The collapse transition has a second order-like behavior and the folding transition seems first order-like. The good folding sequences, i.e., the sequences that are stable and have fast folding times, have sharper, more clearly defined transitions, as viewed from the temperature dependence of the average energy and the specific heat. Combining kinetic and thermodynamic data, we studied the unfolding behavior of the system. The unfolding rate has a much simpler temperature dependence than the folding rate. The rate varies roughly linearly with $1/T$ for a broad range of temperature up to the glass point.

After the density of states was obtained we were not only able to extrapolate to different temperatures but also to different parameter values of the energy function. The systems were examined as a function of the average drive toward compactness, where the average drive is the average of the two contact energies divided (normalized) by their difference (E_{avg}/Δ). There is a specific value for this energy drive at which the kinetic glass temperature became greater than the folding temperature, indicating that the system would no longer be able to fold within the simulation time due to trapping. We constructed a phase diagram as a function of this average drive and temperature (also normalized by the splitting). As the average energy drive is reduced, the two transitions, collapse and folding, converge. At zero-average drive the system collapses almost directly into the native state.

One criticism of these models is that they are too simple to represent real proteins. However, even in this simple model we see a broad and diverse range of behaviors depending on the parameters used. It seems likely that some of the behaviors of real proteins can be explained by some particular set of parameters. More importantly, it may well be the case that different proteins have different folding behaviors. Some proteins may fold extremely rapidly to the native state, literally collapsing into the native state, while other proteins may have a clear separation in time scales between collapse to a compact but non-native ensemble of structures and the rearrangement of the chain to the final native form. In our model we can interpolate between these two regimes by modulating one parameter. In the future, more realistic models that are still simple enough for a thorough analysis may reveal more about the properties and functions of real proteins.

ACKNOWLEDGMENTS

We would like to gratefully acknowledge the computational assistance of A. Schweitzer, W. Bialek and the NEC Research Institute. We thank K. A. Dill, H. S. Chan and P. G. Wolynes for interesting and helpful discussions. We also thank J. Song and A. Schwartz for careful reading of and enlightening comments on the manuscript. N. D. S. is a Chancellor's Fellow at UCSD. J. N. O. is a Beckman Young Investigator. This work was funded by the Arnold and Mabel Beckman Foundation and by the National Science Foundation (Grant No. MCB-9316186).

1. M. Levitt and R. Sharon, *Proc. Natl. Acad. Sci. USA* **85**, 7557 (1988).
2. D. J. Tobias, J. E. Mertz, and C. L. Brooks, *Biochemistry* **30**, 6054 (1991).
3. V. Daggett and M. Levitt, *Proc. Natl. Acad. Sci. USA* **89**, 5142 (1992).
4. M. K. Gilson, T. P. Straatsma, J. A. McCammon, D. R. Ripoll, C. H. Faerman, P. H. Axelsen, and J. L. Sussman, *Science* **263**, 1276 (1994).
5. H. S. Chan and K. A. Dill, *J. Chem. Phys.* **99**, 2116 (1993).
6. H. S. Chan and K. A. Dill, *J. Chem. Phys.* **100**, 9238 (1994).
7. J. D. Bryngelson, J. N. Onuchic, N. D. Soccia, and P. G. Wolynes, *PROTEINS: Structure, Function and Genetics* **21**, 167 (1995).
8. J. N. Onuchic, P. G. Wolynes, Z. Luthey-Schulten, and N. D. Soccia, *Proc. Natl. Acad. Sci. USA* **92**, 3626 (1995).
9. N. D. Soccia and J. N. Onuchic, *J. Chem. Phys.* **101**, 1519 (1994).
10. J. D. Bryngelson and P. G. Wolynes, *Proc. Natl. Acad. Sci. USA* **84**, 7524 (1987).
11. J. D. Bryngelson and P. G. Wolynes, *J. Phys. C* **93**, 6902 (1989).
12. P. E. Leopold, M. Montal, and J. N. Onuchic, *Proc. Natl. Acad. Sci. USA* **89**, 8721 (1992).
13. K. F. Lau and K. A. Dill, *Macromolecules* **22**, 3986 (1989).
14. H. S. Chan and K. A. Dill, *Annu. Rev. Biophys. Biophys. Chem.* **20**, 447 (1991).
15. E. Shakhnovich and A. Gutin, *J. Chem. Phys.* **93**, 5967 (1990).
16. A. Šali, E. Shakhnovich, and M. Karplus, *J. Mol. Biol.* **235**, 1614 (1994).
17. N. Metropolis, A. W. Rosenbluth, M. N. Rosenbluth, A. N. Teller, and E. Teller, *J. Chem. Phys.* **21**, 1087 (1953).
18. A. Sikorski and J. Skolnick, *J. Mol. Biol.* **212**, 819 (1990).
19. J. Skolnick and A. Kolinski, *J. Mol. Biol.* **212**, 787 (1990).
20. J. Skolnick and A. Kolinski, *J. Mol. Biol.* **221**, 499 (1991).

21. E. M. O'Toole and A. Z. Panagiotopoulos, *J. Chem. Phys.* **97**, 8644 (1992).

22. M. N. Rosenbluth and A. W. Rosenbluth, *J. Chem. Phys.* **23**, 356 (1955).

23. E. M. O'Toole and A. Z. Panagiotopoulos, *J. Chem. Phys.* **98**, 3185 (1993).

24. C. J. Camacho and D. Thirumalai, *Proc. Natl. Acad. Sci. USA* **90**, 6369 (1993).

25. A. M. Ferrenberg and R. H. Swendsen, *Phys. Rev. Lett.* **61**, 2635 (1988).

26. A. M. Ferrenberg and R. H. Swendsen, *Phys. Rev. Lett.* **63**, 1195 (1989).

27. The units of temperature and energy are such that $k_b = 1$. This still leaves an arbitrary scale factor since the only important quantity is the ratio of energy to temperature. I.e., we could have picked -200 and 200 for E_{avg} and Δ , multiplied all temperatures by 100 and the results would be the same. We have chosen small, integer values for convenience.

28. P. H. Verdier and W. H. Stockmayer, *J. Chem. Phys.* **36**, 227 (1962).

29. H. J. Hilhorst and J. M. Deutch, *J. Chem. Phys.* **63**, 5153 (1975).

30. K. Kremer and K. Binder, *Comp. Phys. Rept.* **7**, 259 (1988).

31. M. T. Gurler, C. C. Crabb, D. M. Dahlin, and J. Kovac, *Macromolecules* **16**, 398 (1983).

32. Note, in their study (ref. 21) the authors do not attribute the problems with local Monte Carlo moves to a glass transition in the system. However, even though there potential is slightly different than the one used in our study, we feel that their system may also undergoes a glass transition which would explain the hysteresis seen.

33. H. Müller-Krumbhaar and K. Binder, *J. Stat. Phys.* **8**, 1 (1973).

34. N. Madras and A. D. Sokal, *J. Stat. Phys.* **50**, 109 (1988).

35. Assuming that the number of conformations scaled like 3^n (a very conservative underestimate) and that one could enumerate a million conformations every second (a somewhat generous overestimate of computational power) then it would take 29 days to enumerate all conformations. If the number scales like 4^n it would take 142 years.

36. N. A. Alves, B. A. Berg, and R. Villanova, *Phys. Rev. B* **41**, 383 (1990).

37. S. Huang, K. J. M. Moriarty, E. Myers, and J. Potvin, *Z. Phys. C* **50**, 221 (1991).

38. D. Bouzida, S. Kumar, and R. H. Swendsen, *Phys. Rev. A* **45**, 8894 (1992).

39. S. Humar, D. Bouzida, R. H. Swendsen, P. A. Kollman, and J. M. Rosenberg, *J. Comput. Chem.* **13**, 1011 (1992).

40. Actually if one is interested in calculating differences of the free energy then it is not necessary to determine this constant since it will only change the free energy by a additive constant. To see this note that $F = -T \log Z$, so if we know $c * n(E)$ (where $c = 1/Z(T')$ is the constant we do not know) we can get $c * Z$ which gives: $F = -T \log Z + T \log c$.

41. This is a finite time problem (i.e., we must run the simulations of a finite amount of computer time). In the infinite time limit, for a finite system, all regions of phase space would be explored, so the histograms from one temperature could be used to extrapolate to all.

42. E. I. Shakhnovich and A. M. Gutin, *Proc. Natl. Acad. Sci. USA* **90**, 7195 (1993).

43. W. H. Press, B. P. Flannery, S. A. Teukolsky, and W. T. Vetterling, *Numerical Recipes*, Cambridge University Press, New York, 1986.

44. J. D. Hirst and C. L. Brooks, *J. Mol. Biol.* **243**, 173 (1994).

45. A. Li and V. Daggett, *Proc. Natl. Acad. Sci. USA* **91**, 10430 (1994).

46. It is a property of the cubic lattice that there are no conformations of 27 length polymers that have 27 contacts. Therefore for sequences 005, 006, 007, that have 27 or 26 good contacts for some cube, there can be no non-cube conformation with more good contacts. (We no there are no cube conformations with 28 good contacts since we can enumerate all the cubes.) For sequence 013 which only has 24 good contacts it is possible that there is a conformation with 26 good contacts which would give it an energy of -78. However, we have found no such state in the Monte Carlo simulations.

47. Actually for technical reason we ran the various simulation changing the value of E_u leaving the value of E_l fixed at -3. However, data was scaled to unit Δ when plotted by normalizing both the temperature and E_{avg} . E_u was varied from -2 to 3.

48. As mention previously (in note 27) there is an arbitrary scale factor in our unit of energy and temperature. Therefore there are only two independent parameters in our model from the set of three (T , E_{avg} and Δ). We choose to vary T and E_{avg} , and will normalize them to unit Δ .

49. J. D. Bryngelson and P. G. Wolynes, *Biopolymers* **30**, 177 (1990).

50. In their work Bryngelson and Wolynes (see ref. 49) use a slightly different notation and terminology. We discuss the glass transition temperature, T_g they use the term freezing transition and denote the temperature as T_f . This should not be confused what we call the folding temperature (denoted here also as T_f). Also the two transition are different. They calculate a thermodynamic freezing transition while we compute a kinetic transition related to the slow down of the dynamics of the system. See reference 9 for details.

51. E. I. Shakhnovich and A. M. Gutin, *Biophys. Chem.* **34**, 187 (1989).

52. A. Dinner, A. Šali, M. Karplus, and E. Shakhnovich, *J. Chem. Phys.* **101**, 1444 (1994).